Desalination and Water Treatment
www.deswater.com

doi: 10.5004/dwt.2018.23085

129 (2018) 168–176
October

Removal of toxic ammonium ions from water using nanographene sheets

Mohamed Abdel Salam*, Lateefa Alkhateeb, Mohamed A. Abdel-Fadeel

Chemistry Department, Faculty of Science, King Abdulaziz University, P.O. Box: 80200, Jeddah 21589, Saudi Arabia, Tel. +966 541886660; Fax: +966 2 6952292; email: masalam16@hotmail.com (M.A. Salam), Tel. +966 503050614; email: lateefa_2003@hotmail.com (L. Alkhateeb), Tel. +966 596256654; email: m_abdelazeem@hotmail.com (M.A. Abdel-Fadeel)

Received 22 February 2018; Accepted 8 September 2018

ABSTRACT

This paper describes the removal of toxic ammonium ions from model and real water samples using nanographene sheets (NGs). NGs were characterized by using a scanning electron microscope, a transmission electron microscope, X-ray diffraction, and surface area analysis. The results showed that NGs exist as plate-like overlapped transparent wrinkled sheets of graphene with different dimensions and characterized with high Brunauer–Emmett–Teller specific surface area. The effect of different experimental conditions, NGs mass, removal time, solution temperature, and ionic strength, affecting the removal efficiency of NH_4^+ by NGs from synthetic water sample, was studied and optimized. The adsorption experiments showed that NGs could remove most of the ammonium ions within few minutes, with adsorption capacity of 11.6 mg of NH_4^+/g of NGs at ambient conditions. The removal of ammonium ions on NGs was explored kinetically and thermodynamically, and the results revealed the suitability of the pseudo-second-order kinetic model for describing the adsorption process. Also, the adsorption process was spontaneous, exothermic in nature, and negative entropy change indicated the decrease in the degree of freedom at the solid–liquid interface. The applicability of the NGs for the adsorption of ammonium ions was explored using different real environmental water samples, and the results indicated that the NGs have great potential to remove ammonium ions from aqueous solution.

Keywords: Adsorption; Ammonium ions; Kinetics; Nanographene; Thermodynamics, Real water

1. Introduction

Pollution is one of the most serious problems that affect our environment and endanger all living organisms on the earth. Inorganic pollutants are considered among the most important class of pollutants which greatly affects the environment. For example, wastewaters produced from different industries greatly participate in the contamination of the groundwater. These redundant chemicals cause many health and environmental problems, when they exceed tolerance limit in water. Ammonia/ammonium is among the different forms of nitrogen, which are characterized with their solubility in water and can end up in soil, drinking waters, and groundwaters. The presence of ammonium ions (NH_4^+) in the environment could lead to toxicity of various living organisms [1,2] if their concentration exceeds certain limits, as well as eutrophication [3,4]. In accordance with the European legislation, the total nitrogen concentration in municipal sewage plants discharges should be lower than 15 mg N/L in Spain, whereas in Romania, the N-NH^{4+} content in wastewater discharged into water resources should not exceed 2 mg/L, and 15 mg/L in water to be used in irrigation [5], whereas according to Canadian Water Quality Guidelines for the Protection of Aquatic Life, the total ammonia should not exceed 2.77 mg/L total ammonia-N at 25°C and neutral pH [6].

Currently, there are different treatment methods used for removal of toxic ammonium ions from water supplies; including osmosis [7], struvite precipitation process [8], ultrafiltration [9], and adsorption [10–13]. Generally, removal of pollutants such NH_4^+ by adsorption is considered as one of the most effective processes for wastewater treatment without producing any harmful by-products with the possibility

---

* Corresponding author.

of regenerating both pollutants and adsorbent. Nowadays, one of the great challenges in the adsorption technologies is exploring new potential adsorbents which could be used successfully for the removal of different pollutants from aqueous solution [14–17]. Nanoadsorbents are a new class of adsorbents which are used successfully for the removal of different class of pollutants from polluted aquatic environments For example, multi-walled carbon nanotubes (MWCNTs) were used for the removal of different organic compounds [18] and heavy metals [19] from water. Nanographene sheets (NGs) are also another nanoadsorbent which are used for the removal of different pollutants such as organic pollutants, heavy metals, and pathogenic bacteria [20–24] from aqueous solution. NGs are characterized with the high surface area, high adsorption ability due to the presence of the negatively charged π electrons which greatly attract different organic pollutants, and positively charged pollutants such as NH^{4+}.

Although there are many research studies that have reported the removal of NH^{4+} by adsorption process using different adsorption techniques, unfortunately, the application of nanoadsorbent such as NGs has not yet been explored. It is highly expected that NGs will be characterized with high selectivity and efficiency toward the removal of NH^{4+} from solution.

In this research work, NGs were used for the removal of NH^{4+} from aqueous solutions, and real water samples. The NGs were characterized with different chemical and physical techniques, and then different experimental conditions affecting the removal efficiency of NH^{4+} from synthetic water sample were studied and optimized. In addition, the adsorption process will be studied kinetically and thermodynamically to understand the mechanism of removal and spontaneity in order to enhance the efficiency of the removal process.

2. Experimental procedures

2.1. Reagents and materials

All chemicals and solvents used were of analytical reagent-grade quality and were used without further purification. NGs were obtained from XG Science (xGnP® 300, USA) and were used as received. A stock of standard ammonia solution, 1,000 mg/L, was prepared from ammonium chloride (Fluka A G) by dissolving appropriate amount of ammonium chloride in deionized water. A diluted standard ammonia sample solution, 10 mg/L, was prepared by diluting the stock solution with deionized water. Solution (1) was prepared by dissolving phenol (25 g) and sodium nitroprusside (125 mg) (BDH chemicals, Poole, England) in 500 mL of deionized water, and Solution (2) was prepared by dissolving sodium hydroxide (12 g) and sodium hypochlorite (1.05 g) (Fluka A G) in 500 mL of deionized water.

2.2. Characterization techniques

Scanning electron microscopy (SEM) image for the NGs was obtained using a Quanta 600 FEG SEM from FEI Company, USA. Nanostructure morphology of the NGs was measured using JEOL-JEM-1230 (Japan) transmission electron microscopy (TEM). The sample was suspended in ethanol and ultrasonicated for 30 min. A small amount of the NGs was then dried on a carbon-coated copper grid and loaded into the TEM. The X-ray diffraction (XRD) pattern of the NGs was collected on a Bruker (Germany) DMAX 2500 X-ray diffractometer equipped with a Cu Kα radiation source (λ = 0.154 nm). The N_2 adsorption/desorption isotherms for the NGs were conducted using a Micrometrics (USA) ASAP 2420 to determine the Brunauer–Emmett–Teller (BET) surface area. The zeta potential measurement of the NGs in an aqueous dispersion was performed on Malvern, Zetasizer Nano, ZS90. 5.0 mg of the NGs were ultrasonicated and suspended for 30 min in 100 mL of water, then the pH of the suspension was then adjusted between 2 and 11 using 0.1 M HCl or 0.1 M NaOH solution. The pH value where the zeta potential was zero was taken as the point of zero charge.

2.3. Adsorption experiment

A defined mass of the NGs was equilibrated with an aqueous solution (10 mL) containing NH_4^+ (10 mg/L), and the solution was then shaken for 1 h using a JULABO SW23 shaking water bath with thermostatic control. The aqueous phase was then separated out using Millipore® (Germany) filtration system with membrane filter of 10.0 μm, and the amount of NH_4^+ remaining in the aqueous phase was determined spectrophotometrically using indophenol method at wavelength 630 nm using Solution 1 and Solution 2 [25]. The percentage of adsorption expressed as % (Eq. (1)), and the amount of ammonium ions adsorbed (q_t) per unit mass of NGs (mg of NH_4^+/g) (Eq. (2)), were finally calculated according to the following:

$$\text{Adsorption}(\%) = \frac{C_0 - C_t}{C_0} \times 100(\%) \tag{1}$$

$$q_t = \frac{(C_0 - C_t)V}{m} \tag{2}$$

where C_0 and C_t are the initial and final concentrations of NH_4^+ in solution (mg/L), respectively, V is the volume of the solution (L), and m is the mass of the NGs used (g). It is noteworthy to mention that all the experiments were repeated three times, and the reported values represent the averages.

2.4. Environmental applications and sample collection

Three real water samples were collected to evaluate the efficiency of NGs for the removal of ammonium ions, tap water, waste water, and sea water samples. The tap water sample was collected from the laboratories of Chemistry Department, King Abdulaziz University, Jeddah city (Latitude deg. North 21.497192, Longitude deg. East 39.249140), the wastewater sample was collected from the Membrane Bio-Reactor Technology Waste Water Treatment Plant (MBR 6000 STP) at King Abdulaziz University, Jeddah city (Latitude deg. North 21.487954, Longitude deg. East 39.236748), and the sea water sample was collected from the Red Sea in front of Jeddah city (Latitude deg. North 21.518333, Longitude deg. East 39.150677), and the samples were filtered through 0.45 μm membrane and kept in Teflon bottles in the dark at 5°C.

3. Results and discussions

3.1. Characterization of the nanographene

The surface morphology of the NGs was investigated using SEM imaging, and as it is clear from Fig. 1, NGs exists as plate-like overlapped layered microstructure with different dimensions. Also; as shown in Fig. 2, TEM image of the NGs showed the transparent wrinkled overlapped sheets of NGs with different length and width. The crystallinity and verification of the NGs was determined using XRD. The diffraction peaks at 2θ angles of 26.3°–54.1° in the XRD pattern of NGs confirm their identity as nanosheets of graphene same as that of native graphite (JCPDS No. 08-0415), as it is presented in Fig. 3. Moreover, the reflection peaks of the NGs could be attributed to the hexagonal phase carbon with space group of P63/mmc. Fig. 4 shows the N_2 adsorption/desorption isotherms of the NGs at 77 K. The specific surface area for the NGs was estimated using the BET equation and was 279 m^2/g. Moreover, it is noteworthy to mention that the adsorption/desorption isotherm of the NGs could be classified as a Type II isotherm with an H3-type hysteresis loop confirming the presence of the NGs in the form of non-rigid aggregates of plate-like industrial adsorbents, according to the recent IUPAC classification [26].

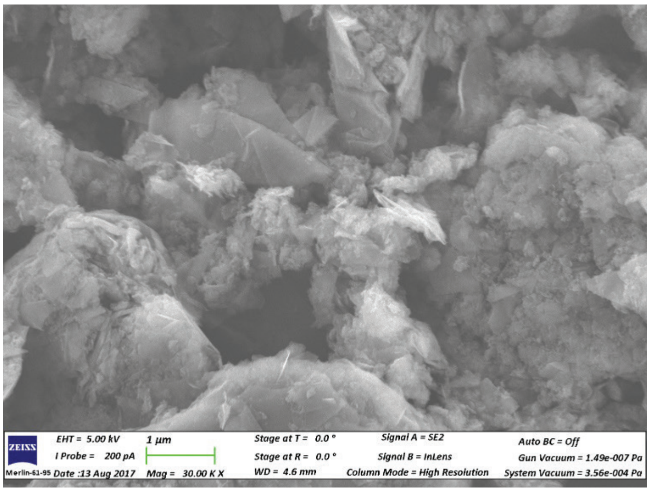

Fig. 1. Representative scanning electron microscope image for NGs.

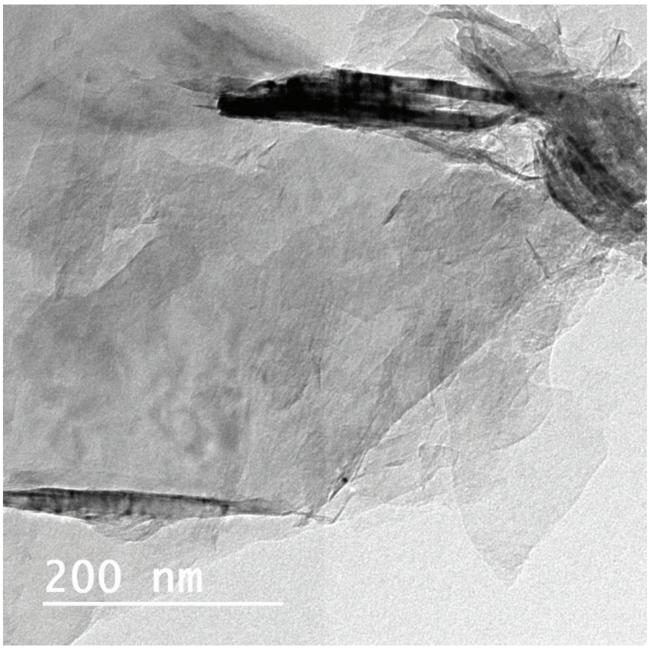

Fig. 2. Transmission electron microscope image of NGs.

3.2. Adsorption study

Adsorption of pollutants from water by solid adsorbent depends on different factors, such as adsorbent mass, contact time, solution temperature, and ionic strength [27,28]. Therefore, the effect of these parameters on the removal of NH_4^+ by NGs from an aqueous solution was investigated in order to achieve better understanding of the removal process and accomplished the highest efficacy.

The adsorbent mass is one of the crucial parameters in the adsorption process, as it determines the adsorbent capacity for a given initial concentration of pollutant in a solution. Accordingly, the adsorption profile of the aqueous solution containing NH_4^+ with concentration 10 mg/L at different mass of NGs was studied after shaking for 60 min at room temperature, and the results are shown in Fig. 5. The experimental

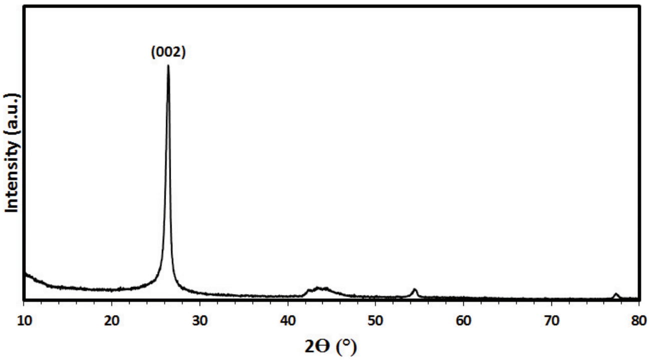

Fig. 3. XRD pattern of NGs.

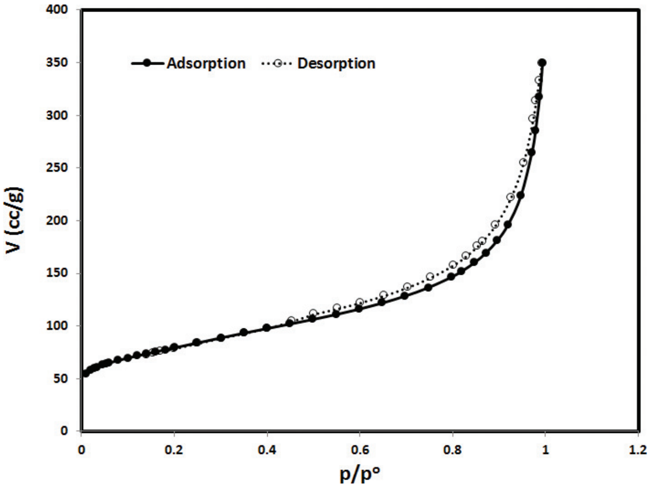

Fig. 4. Adsorption/desorption isotherms for NGs using nitrogen at 77 K.

results indicated that the percentage of NH_4^+ removed from the aqueous solution gradually increased from 58.0% to 99.0% as the NGs mass increased from 5 to 20 mg, which attributed to the presence of larger number of active sites accessible for adsorption due to the greater amount of NGs present. Hence, in this research work, 5 mg NGs, which corresponded to 58%, is to be able to observe the effect of other parameters on the adsorption process.

The contact time between the adsorbate and the solid adsorbent is another key factor affecting the removal of any pollutants from the environment via adsorption process. Consequently, the effect of the contact time on the removal of NH_4^+ by NGs was studied, and the results are shown in Fig. 6. The figure shows that increasing the contact time led to a gradual increase of the adsorption percentage within the first 15 min. At contact time longer than 15 min, a slow increase in the adsorption of NH_4^+ by NGs was observed, and equilibrium was attained within 30 min. This indicates the adsorption of NH_4^+ by NGs occurred in two consecutive steps, the first one, was the fastest, which could be attributed to the transfer of NH_4^+ from aqueous phase to the external surface of NGs, followed by a slower step, attributed to the diffusion of NH_4^+ between the NGs sheets.

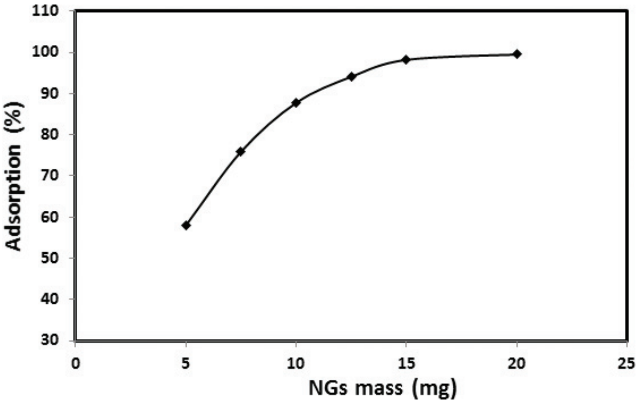

Fig. 5. Effect of NGs mass on the adsorption percentage of ammonium ions from aqueous solution onto NGs.

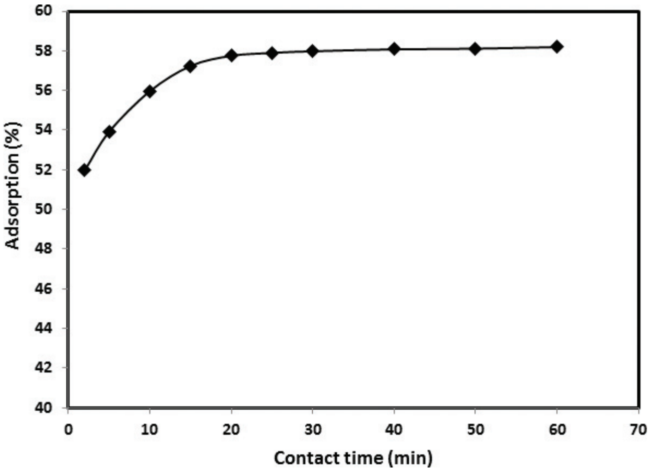

Fig. 6. Effect of shaking time on the adsorption percentage of ammonium ions from aqueous solution onto NGs.

The solution temperature is another factor which greatly affect the removal of pollutants from aqueous solution by solid adsorbent, as it greatly affects the diffusion/transfer of the adsorbate ions/molecules in solution, thus, the effect of solution temperature on the adsorption of NH_4^+ by NGs was investigated at four different temperatures, 293, 303, 313 and 323 K, and the solution temperature was adjusted and preserved to the desired temperature using the shaking water bath with thermostatic control. It was observed that raising the solution temperature from 293 to 323 K was significantly associated with a significant decrease in the percentage of NH_4^+ adsorbed by the NGs as it is presented in Fig. 7. These results suggest an exothermic nature of the adsorption of NH_4^+ by the NGs, which will be discussed thoroughly at the thermodynamics study section.

Influence of the ionic strength on the adsorption of pollutants in aqueous solution by solid adsorbent is very important as it can create different adsorption situations by which electrostatic interactions between the solid adsorbent surface and pollutant are either attractive or repulsive in nature. The ionic strength of the solution of the NH_4^+ solution was adjusted using different concentrations of KNO_3, 0.005, 0.01, 0.5, and 0.1 M, and their effect on the adsorption process by NGs was explored, and presented in Fig. 8. The results showed that the adsorption percentage was gradually increased with the increase of the ionic strength of the solution. The observed

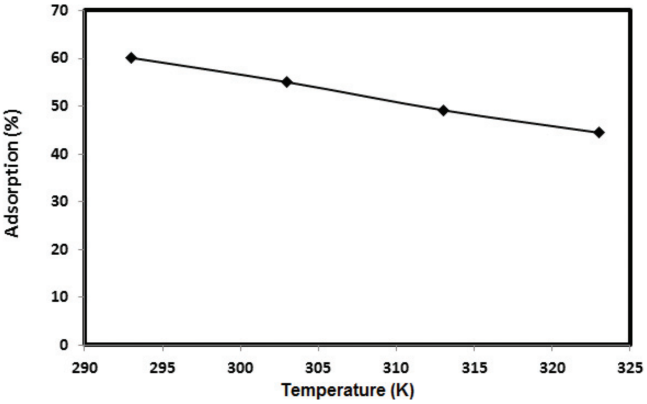

Fig. 7. Effect of temperature on the adsorption percentage of ammonium ions from aqueous solution onto NGs.

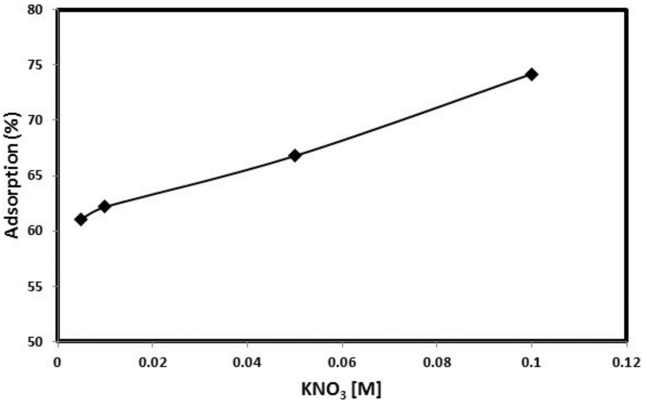

Fig. 8. Effect of KNO_3 concentration on the adsorption of ammonium ions from aqueous solution by NGs.

increases in the percentage adsorption could be explained by the attractive nature of the electrostatic interactions between the NH_4^+ and the NGs surface, as the surface of the NGs were negatively charged (point of zero charge equals 3.4), and as the experiments were conducted at neutral pH value of 7.0. Also, it is noteworthy to mention that a double layer around the NGs surface formed upon the addition of the KNO_3, where the positive potassium ions (K^+) attracted first to the surface of the negatively charged NGs forming the first layer, followed by the formation of the second layer of the negatively charged nitrate ions (NO_3^-), which make the surface of the NGs by the addition of the KNO_3 more negative, which greatly enhanced the attractive nature of the electrostatic interactions between the NH_4^+ and the NGs surface.

Accordingly, 99.0% of the ammonium ions could be efficiently removed, at a 10 mg/L ammonium ions concentration, using 2.0 mg NGs per mL within 60 min shacking time, pH 7.0.0, and temperature at 293 K.

3.3. Kinetic study

The study of the adsorption kinetic of pollutants such as NH_4^+ in water using solid adsorbent such as NGs is of great importance to understand the interaction mechanism and pathways. Fig. 9(a) shows that the adsorption experimental data represent the variation of the amount NH_4^+ adsorbed from aqueous solution by NGs (q_t) with time, and results showed that the equilibrium was attained within 30 min with maximum adsorption capacity of 11.64 mg NH_4^+/g NGs. The adsorption experimental data were treated kinetically using the most common and well-known kinetic models in order to understand the nature of the adsorption process, fractional power function model [29], Lagergren pseudo-first-order kinetic model [30], and pseudo-second-order kinetic model [31].

Eq. (3) shows the linearized form of the fractional power function kinetic model:

$$\ln q_t = \ln a + b \ln t \tag{3}$$

where q_t (mg/g) is the amount of NH_4^+ adsorbed per unit mass of NGs at any time t, while a and b are coefficients with $b < 1$. Applying the fractional power function kinetic model equation to the experimental data in Fig. 9(b) did not converge well and low correlation coefficient (R^2) value of 0.914 was obtained, as it is presented in Table 1, indicating the inappropriateness of the fractional power function kinetic model for description of NH_4^+ adsorption by the NGs.

Lagergren pseudo-first-order kinetic model is a very common model used to describe the adsorption of different adsorbates from an aqueous solution by solid adsorbent:

$$\ln(q_e - q_t) = \ln q_e - k_1 t \tag{4}$$

where k_1 (min^{-1}) is the pseudo-first-order adsorption rate coefficient, and q_e and q_t are the values of the amount adsorbed per unit mass at equilibrium and at any time t, respectively. Applying Eq. (4) to the experimental adsorption data in Fig. 9(a) and by plotting ln (q_e–q_t) vs. t did not converge well, and low R^2 value of 0.925 was obtained, as it is shown in Fig. 9(c) and Table 1, showing clearly the unsuitability of Lagergren pseudo-first-order kinetic model for describing the removal of the NH_4^+ from aqueous solution onto NGs.

The linearized equation of the pseudo-second-order kinetic model equation is given as follows:

$$\frac{t}{q_t} = \frac{1}{k_2 q_e^2} + \frac{t}{q_e} \tag{5}$$

where k_2 (g/(mg·min)) is the pseudo-second-order rate coefficient. Applying the pseudo-second-order kinetic model equation to the data in Fig. 9(a), and by plotting of t/q_t and t of Eq. (5), a straight line was obtained, with excellent R^2 value of 0.999 was obtained as it is presented in Fig. 9(d) and Table 1, validating the applicability of the pseudo-second-order kinetic model for the description of the NH_4^+ removal from aqueous solution by NGs indicating that each adsorbed NH_4^+ is attached to two active negative sites at the NGs surface, the adsorption may involve valency forces through sharing or exchange of electrons between NGs and NH_4^+ ions, which is not the case with the pseudo-second-order kinetic model [32]. The suitability of the pseudo-second-order kinetic model was examined by performing the Chi-square test [33]:

$$\chi^2 = \sum \frac{(q_{e,\text{calc}} - q_{e,\text{exp}})^2}{q_{e,\text{calc}}} \tag{6}$$

where $q_{e,\text{exp}}$ and $q_{e,\text{calc}}$ are the calculated and experimental amount of NH_4^+ adsorbed per unit mass of NGs at equilibrium, respectively. Accordingly, the χ^2 values for the pseudo-first and pseudo-second-order kinetic models were 137.9 and 0.0001, respectively, confirming the suitableness of the pseudo-second-order kinetic model for the description of NH_4^+ adsorption by NGs.

The removal of adsorbate such as NH_4^+ by solid adsorbent such as NGs from aqueous solution takes place in four sequential steps. Firstly, the transport of NH_4^+ from the bulk solution to the external surface of the NGs, which is followed by their diffusion through the liquid film surrounding the external surface of NGs, then adsorption of the NH_4^+ at an active site on the NGs surface, and at the end, diffusion of the ions through the NGs aggregates, intra-particle diffusion. Accordingly, liquid film [34] and intra-particle [35] diffusion models for the adsorption of NH_4^+ onto NGs from aqueous solution were explored mechanistically.

The liquid film diffusion model could be expressed as the following:

$$\ln(1 - F) = -k_{\text{fd}} \times t \tag{7}$$

where F is the fractional attainment of equilibrium ($F = q_t/q_e$) and k_{fd} (min^{-1}) is the film diffusion rate coefficient. Applying the liquid film diffusion model to all the experimental adsorption data in Fig. 9(a), by plotting of ln(1–F) vs. t with zero intercept, did not converge well as it is presented in Fig. 9(e), suggesting that the adsorption process was not controlled by the diffusion of the NH_4^+ through the liquid film around the NGs.

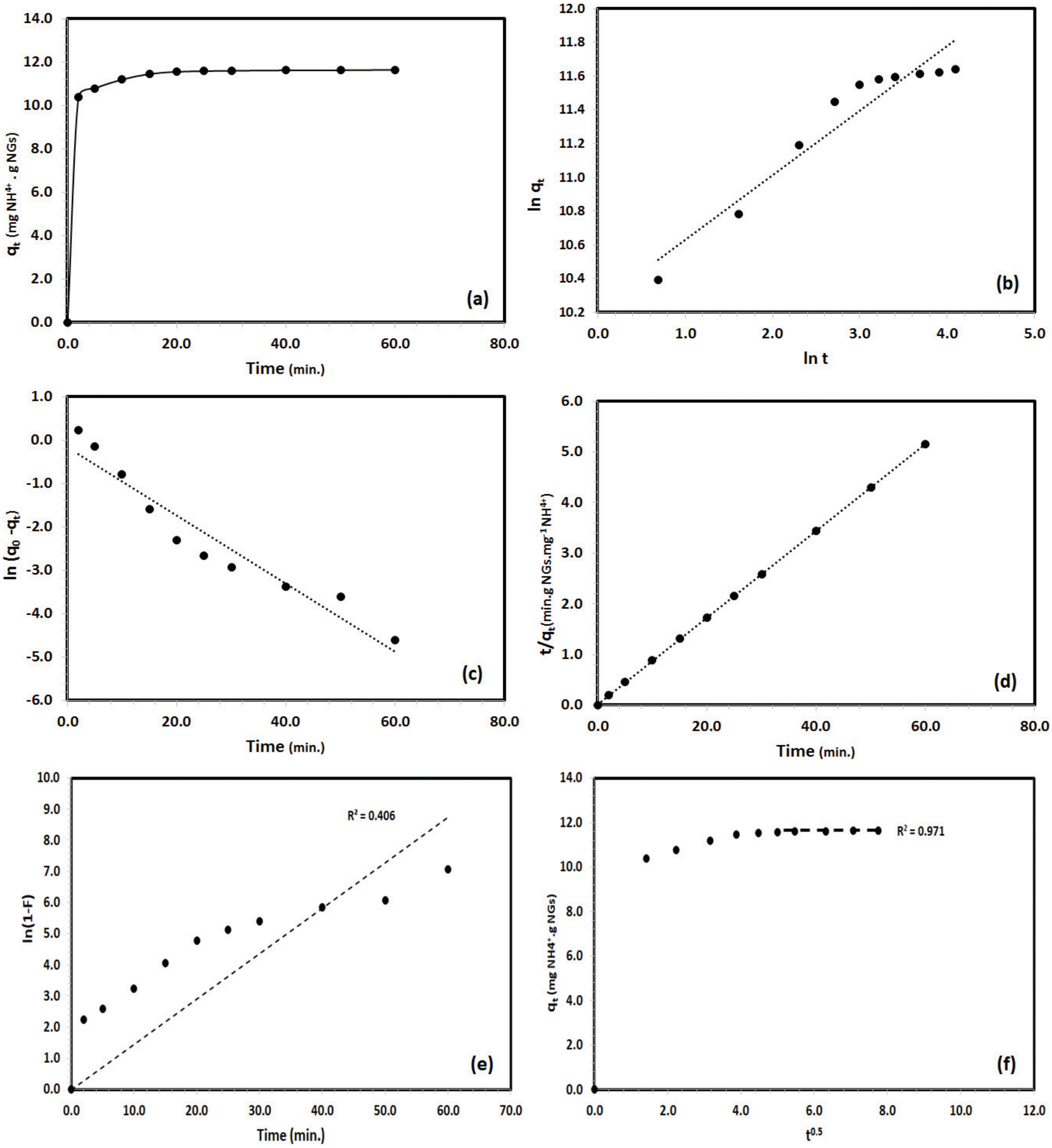

Fig. 9. (a) Variation of the amount of ammonium ions adsorbed per unit mass of NGs (q_t) with time, (b) the application of fractional power function model, (c) Lagergren pseudo-first-order kinetic model, (d) pseudo-second-order kinetic model, (e) liquid film diffusion model, and (f) intra-particle diffusion model for the ammonium ions removed from an aqueous solution by NGs.

Intra-particle diffusion model could be expressed as the following:

$$q_t = k_{\mathrm{id}} t^{1/2} + C \tag{8}$$

where k_{id} is the intra-particle diffusion rate constant (mg/g min$^{1/2}$) and C (mg/g) is a constant proportional to the thickness of the boundary layer. Applying the intra-particle diffusion model to all the adsorption experimental data in Fig. 9(a) with zero intercept did not converge well and did not have straight lines pass through the origin as well as it is presented in Fig. 9(f), which repudiate the suitability of the intra-particle diffusion model for all the experimental data. As it was explained earlier, the last step of the adsorption process is the intra-particle diffusion through the pores and aggregates of the NGs, therefore, the intra-particle diffusion equation was applied to the last 35 min of experimental adsorption data. Surprisingly, the intra-particle diffusion equation fitted well and converged with the last adsorption data in the time range between 25 and 60 min as predicted, with good R^2 value of 0.971, as it is presented in Fig. 9(f) and Table 1.

A comparison of the adsorption capacities of different solid adsorbents used in previous studies and the NGs used in this work was performed and represented in Table 2. It is clear from the table that NGs are a potential and competitive adsorbent for the removal of ammonium ions from aqueous solution.

3.4. Thermodynamic studies

The removal of NH_4^+ by NGs was studied thermodynamically at different temperature, and the enthalpy change ($\Delta H°$), entropy change ($\Delta S°$), and Gibbs free energy change ($\Delta G°$), were calculated to evaluate the thermodynamic feasibility and the spontaneity of the adsorption process. Thermodynamic parameters were calculated using the following equations [36]:

$$K_c = \frac{C_A e}{C_e} \tag{9}$$

$$\Delta G° = -RT \ln K_c \tag{10}$$

$$\Delta G° = \Delta H° - T\Delta S° \tag{11}$$

$$\ln K_c = \frac{\Delta S°}{R} - \frac{\Delta H°}{RT} \tag{12}$$

where C_e is the equilibrium concentration of NH_4^+ in solution (mg/L), $C_A e$ is the amount of NH_4^+ adsorbed on the NGs per liter of solution at equilibrium (mg/L), R is the gas constant (8.314 J/mol K), T is the temperature (K), and K_c is the equilibrium constant. The values of $\Delta H°$ and $\Delta S°$ were calculated from the slope and the intercept of the plot of ln K_c vs. $1/T$ as it is presented in Fig. 10.

Table 1
The parameters of different kinetic models used for the description of ammonium ions removal onto NGs from an aqueous solution

Fractional power kinetic model			
A	b	ab	R^2
10.26	0.0345	0.354	0.914
Pseudo-first-order kinetic model			
k_1	$q_{e,\,\mathrm{exp}}$ (mg/g)	$q_{e,\,\mathrm{calc}}$ (mg/g)	R^2
0.078	11.65	0.846	0.925
Pseudo-second-order kinetic model			
k_2 (g/mg.min)	$q_{e,\,\mathrm{exp}}$ (mg/g)	$q_{e,\,\mathrm{calc}}$ (mg/g)	R^2
0.326	11.65	11.68	0.999
Liquid film diffusion model			
k_{fd} (min^{-1})		R^2	
2.03		0.833	
Intra-particle diffusion model			
k_d (mg/g min$^{1/2}$)		C (mg/g)	R^2
0.020		11.48	0.971

Thermodynamic parameters for the adsorption of NH_4^+ adsorbed by the NGs were calculated, and $\Delta H°$, $\Delta S°$, and $\Delta G°$ values were –16.8 kJ/mol, –53.8 J/mol K, and –0.744 kJ/mol, respectively. The negative value of the $\Delta H°$ indicated the exothermic nature of the NH_4^+ at the NGs surface, and the negative value of the $\Delta S°$ indicated the decrease in the degree of freedom at the solid–liquid interface due to the immobilization of NH_4^+ on the NGs surface, and apparently the negative value of the $\Delta G°$, at 298 K, as would be expected for a product favored and spontaneous adsorption process. Accordingly, the negative values of $\Delta G°$, $\Delta H°$, and $\Delta S°$ suggested that

Table 2
A comparison of the adsorption capacities of different solid adsorbents for the removal of ammonium ions from an aqueous solution

Adsorbent	Adsorption capacity (mg/g)	Reference
Current work	11.6	This work
SDS modification of AC	1.75	[38]
Natural Chinese zeolite	2.89	[39]
Coconut shell-AC	2.48	[40]
Composite	24.8	[41]
Zeolite	16.0	[41]
Activated carbon	6.89	[41]
Graphene laminate electrodes	15.3	[42]
MWCNTs	9.31	[43]
Posidonia oceanica fibers	1.73	[44]
Zeolite 13X	8.61	[45]
Natural bentonite	26.63	[46]
Vermiculite clay mineral	50.1	[47]
Halloysite clay mineral	9.97	[47]

SDS, Sodium dodecyl sulfate; AC, modified activated carbon.

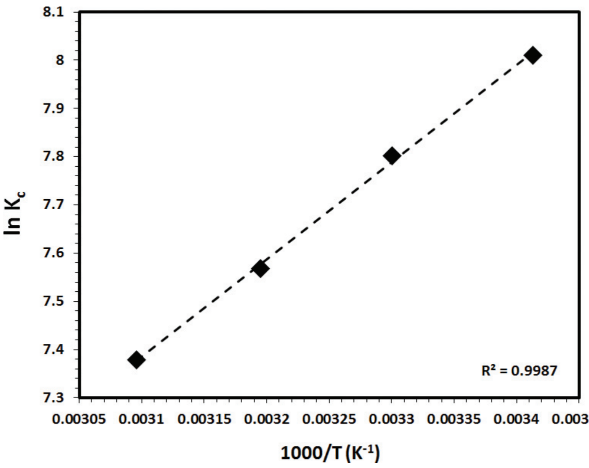

Fig. 10. Plot of ln K_c vs. 1,000/T for the thermodynamic study of ammonium ions adsorption from an aqueous solution by NGs.

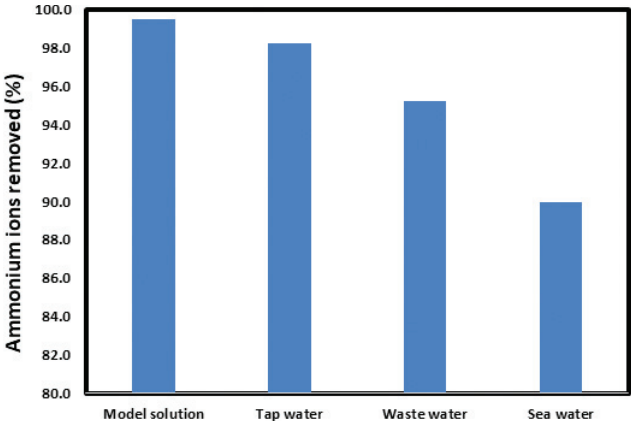

Fig. 11. The removal percentages of ammonium ions from different real water samples by NGs.

the removal of NH_4^+ by the NGs from aqueous solution is a spontaneous enthalpy-driven process. Also, the $\Delta H°$ value indicating that the adsorption process is physical in nature as the value is less than 40 kJ/mole [37].

3.5. Environmental applications

To study the applicability of NGs for the removal of NH_4^+ from real environmental samples were used. The concentration of NH_4^+ was measured for three samples and was found to be lower than the detection limit of the UV–Vis spectrophotometer. Therefore, the three samples were spiked with ammonium ions to obtain a final concentration of 10 mg/L. The percentages of NH_4^+ removed from the real samples were found to be 98.2% for tap water, 95.2% for the waste water, and 89.9% for the sea water, as it is presented in Fig. 11. Then, the NGs were collected, washed with acetone, dried, and reused for the removal of NH_4^+, and almost the same percentage of removal was obtained for four consecutive cycles. This validates the ability to recycle and reuse NGs for a number of removal cycles without losing its efficiency.

4. Conclusions

The removal of the toxic ammonium ions from an aqueous solution was explored using NGs. The solid adsorbent NGs was characterized using SEM, TEM, XRD, and surface area analyzer, and the results showed that NGs exist as plate-like overlapped transparent wrinkled sheets of graphene with different dimensions, and characterized with BET specific surface area of 279 m^2/g. The effect of different experimental conditions on the removal of ammonium ions from an aqueous solution by NGs was explored, and the results revealed that at a 10 mg/L ammonium ions concentration, 99.0% of the ammonium ions could be efficiently removed using 2.0 mg NGs per mL within 60 min shacking time, pH 7.0.0, and temperature at 293 K. Also, the results showed also that the interaction of the ammonium ions with the NGs was physical and electrostatic in-nature. The removal of NH_4^+ by NGs was studied kinetically using different kinetic models and the pseudo-second-order model was the most suitable model as it is characterized by the highest correlation coefficient, as well as the lowest Chi-square value. The removal process was studied thermodynamically, and the results revealed that the removal was spontaneous, exothermic in nature, and associated with negative entropy value. Finally, the NGs was used for the removal of ammonium ions from three different real environmental water samples collected, and the results showed the high efficiency of the NGs for the removal of ammonium ions for four consecutive cycles. These results showed that NGs could be used efficiently for the removal of pollutants from an aqueous solution.

Acknowledgment

The project was funded by the Saudi Basic Industries Corporation (SABIC) and the Deanship of Scientific Research (DSR) at King Abdulaziz University, Jeddah, under grant no. (S-339-130-37). The authors, therefore, acknowledge with thanks SABIC and DSR for technical and financial support.

References

[1] X. Zheng, K. He, T. Kleisti, F. Chen, S. Luan, Anion channel SLAH3 functions in nitrate-dependent alleviation of ammonium toxicity in *Arabidopsis*, Plant Cell Environ., 38 (2015) 474–486.
[2] M.E. Ortiz-Santaliestra, A. Marco, Influence of dissolved oxygen conditions on toxicity of ammonium nitrate to larval natterjack toads, Arch. Environ. Contam. Toxicol., 69 (2015) 95–103.
[3] X. Zhu, Q. Wang, L. Zhang, J. Liu, C. Zhu, Z. Yang, Offspring performance of *Daphnia magna* after short-term maternal exposure to mixtures of microcystin and ammonia, Environ. Sci. Pollut. Res., 22 (2015) 2800–2807.
[4] B. Dunck, E. Lima-Fernandes, F. Cássio, A. Cunha, L. Rodrigues, C. Pascoal, Responses of primary production, leaf litter decomposition and associated communities to stream eutrophication, Environ. Pollut., 202 (2015) 32–40.
[5] E. Marañón, M. Ulmanu, Y. Fernández, I. Anger, L. Castrillón, Removal of ammonium from aqueous solutions with volcanic tuff, J. Hazard. Mater., 137 (2006) 1402–1409.
[6] Canadian Water Quality Guidelines for the Protection of Aquatic Life. Available at: http://ceqg-rcqe.ccme.ca/download/en/141.
[7] X. Li, Y. Lu, Z. He, Removal of reverse-fluxed ammonium by anammox in a forward osmosis system using ammonium bicarbonate as a draw solute, J. Membr. Sci., 495 (2015) 424–430.
[8] A. Escudero, F. Blanco, A. Lacalle, M. Pinto, Struvite precipitation for ammonium removal from anaerobically treated effluents, J. Environ. Chem. Eng., 3 (2015) 413–419.
[9] F. Tortora, V. Innocenzi, M. Prisciandaro, Ida De Michelis, F. Vegliò, G.M. di Celso, Removal of tetramethyl ammonium hydroxide from synthetic liquid wastes of electronic industry through micellar enhanced ultrafiltration, J. Disperion Sci. Technol., 39 (2018) 207–213.
[10] K. Zare, H. Sadegh, R. Shahryari-ghoshekandi, M. Asif, I. Tyagi, S. Agarwal, V.K. Gupta, Equilibrium and kinetic study of ammonium ion adsorption by Fe_3O_4 nanoparticles from aqueous solutions, J. Mol. Liq., 213 (2016) 345–350.
[11] Z. Ahmed, K. Kim, J. Shin, Kinetic, thermodynamic, and equilibrium studies for adsorption of ammonium ion on modified polyurethane, Desal. Wat. Treat., 57 (2016) 14849–14857.
[12] Y. Angar, N. Djelali, S. Kebbouche-Gana, Kinetic and thermodynamic studies of the ammonium ions adsorption onto natural Algerian bentonite, Desal. Wat. Treat., 57 (2016) 25696–25704.
[13] Y. Zhao Y. Niu, X. Hu, B. Xi, X. Peng, W. Liu, W. Guan, L. Wang, Removal of ammonium ions from aqueous solutions using zeolite synthesized from red mud, Desal. Wat. Treat., 57 (2016) 4720–4731.
[14] P.S. Kumar, R. Sivaranjanee, U. Vinothini, M. Raghavi, K. Rajasekar, K. Ramakrishnan, Adsorption of dye onto raw and

surface modified tamarind seeds: isotherms, process design, kinetics and mechanism, Desal. Wat. Treat., 52 (2014) 2620–2633.

[15] P.S. Kumar, J. Pavithra, S. Suriya, M. Ramesh, K. Anish Kumar, *Sargassum wightii*, a marine alga is the source for the production of algal oil, bio-oil, and application in the dye wastewater treatment, Desal. Wat. Treat., 55 (2015) 1342–1358.

[16] P.S. Kumar, S.J. Varjani, S. Suganya, Treatment of dye wastewater using an ultrasonic aided nanoparticle stacked activated carbon: kinetic and isotherm modelling, Bioresour. Technol., 250 (2017) 716–722.

[17] S. Suganya, P.S. Kumar, A. Saravanan, P.S. Rajan, C. Ravikumar, Computation of adsorption parameters for the removal of dye from wastewater by microwave assisted sawdust: theoretical and experimental analysis, Environ. Toxicol. Pharmacol., 50 (2017) 45–57.

[18] C. Jung, A. Son, N. Her, K.-D. Zoh, J. Cho, Y. Yoon, Removal of endocrine disrupting compounds, pharmaceuticals, and personal care products in water using carbon nanotubes: a review, J. Ind. Eng. Chem., 27 (2015) 1–11.

[19] G. Bhanjana, N. Dilbaghi, K.-H. Kim, S. Kumar, Carbon nanotubes as sorbent material for removal of cadmium, J. Mol. Liq., 242 (2017) 966–970.

[20] M. Abdel Salam, Adsorption of nitroaniline onto high surface area nanographene, J. Ind. Eng. Chem., 28 (2015) 67–72.

[21] L.A. Al-Khateeb, W. Hakami, M. Abdel Salam, Removal of non-steroidal anti-inflammatory drugs from water using high surface area nanographene: kinetic and thermodynamic studies, J. Mol. Liq., 241 (2017) 733–741.

[22] A. Taufik, R. Saleh, Organic dyes removal using magnetic $Fe_3O_4^-$ nanographene platelets composite materials, Physica B, 526 (2017) 166–171.

[23] A.A. Yakout, D. Abd El-Hady, H.M. Albishri, M.A Shaker, A.H. Abdel-Salam, A.S. El-Ahl, M.E.S. Ali, Solvothermal magnetic graphene oxide for efficient and fast remediation of p-nitroaniline from industrial wastewaters, Asian J. Chem., 29 (2017) 175–180.

[24] S. Zhan, D. Zhu, S. Ma, W. Yu, Y. Jia, Y. Li, H. Yu, Z. Shen, Highly efficient removal of pathogenic bacteria with magnetic graphene composite, ACS Appl. Mater. Interfaces, 25 (2015) 4290–4298.

[25] Z. Marczenko, Separation and Spectrophotometric Determination of Elements, 2nd ed., John Wiley & Sons, 1986.

[26] M. Thommes, K. Kaneko, A.V. Neimark, J.P. Olivier, F. Rodriguez-Reinoso, J. Rouquerol, K.S.W. Sing, Physisorption of gases, with special reference to the evaluation of surface area and pore size distribution (IUPAC Technical Report), Pure Appl. Chem., 87 (2015) 1051–1069.

[27] R.T. Yang, Adsorbents: Fundamentals and Applications, John Wiley & Sons, Hoboken, New Jersey, 2003.

[28] K.E. Noll, V. Gounaris, W. Hou, Adsorption Technology for Air and Water Pollution Control, CRC Press, Chelsea, Michigan, 1991.

[29] R.C. Dalal, Desorption of soil phosphate by anion-exchange resin, Commun. Soil Sci. Plant Anal., 5 (1974) 531–538.

[30] S. Lagergren, Zur theorie der sogenannten adsorption gel.oster Stoffe – about the theory of so-called adsorption of soluble substances, K. Sven. Vet. Akad. Handl., 24 (1898) 1–39.

[31] W. Rudzinski, W. Plazinski, On the applicability of the pseudo-second order equation to represent the kinetics of adsorption at solid/solution interfaces: a theoretical analysis based on the statistical rate theory, Adsorption, 15 (2009) 181–192.

[32] Y.S. Ho, G. McKay, Pseudo-second order model for sorption processes, Process Biochem., 34 (1999) 451–465.

[33] V. Bagdonavicius, M.S. Nikulin, Chi-square goodness-of-fit test for right censored data, Int. J. Appl. Math., 24 (2011) 30–50.

[34] G.E. Boyd, A.W. Adamson, L.S. Myers, The exchange adsorption of ions from aqueous solutions by organic zeolites II kinetics, J. Am. Chem. Soc., 69 (1947) 2836–2848.

[35] W.J. Weber, J.C. Morris, Kinetics of adsorption on carbon from solution, J. Sanit. Eng. Div. Am. Soc. Civil Eng., 89 (1963) 31–60.

[36] S. Suganya, P.S. Kumar, Kinetic and thermodynamic analysis for the redemption of effluents containing Solochrome Black T onto powdered activated carbon: a validation of new solid-liquid phase equilibrium, J. Mol. Liq., 259 (2018) 88–101.

[37] H. Nollet, M. Roels, P. Lutgen, P. Van der Meeren, W. Verstraete, Removal of PCBs from wastewater using fly ash, Chemosphere, 53 (2003) 655–665.

[38] W. Lee, S. Yoon, J.K. Choe, M. Lee, Y. Choi, Anionic surfactant modification of activated carbon for enhancing adsorption of ammonium ion from aqueous solution, Sci. Total Environ., 639 (2018) 1432–1439.

[39] H. Huang, X. Xiao, B. Yan, L. Yang, Ammonium removal from aqueous solutions by using natural Chinese (Chende) zeolite as adsorbent, J. Hazard. Mater., 175 (2010) 247–252.

[40] R. Boopathy, S. Karthikeyan, A.B. Mandal, G. Sekaran, Adsorption of ammonium ion by coconut shell-activated carbon from aqueous solution: kinetic, isotherm, and thermodynamic studies, Environ. Sci. Pollut. Res., 20 (2013) 533–542.

[41] A.A. Halim, H.A. Aziz, M.A.M. Johari, K.S. Ariffin, Comparison study of ammonia and COD adsorption on zeolite, activated carbon and composite materials in landfill leachate treatment, Desalination, 262 (2010) 31–35.

[42] Y. Wimalasiri, M. Mossad, L. Zou, Thermodynamics and kinetics of adsorption of ammonium ions by graphene laminate electrodes in capacitive deionization, Desalination, 357 (2015) 178–188.

[43] O. Moradi, Applicability comparison of different models for ammonium ion adsorption by multi-walled carbon nanotube, Arabian J. Chem., 9 (2016) S1170–S1176.

[44] S. Jellali, M.A. Wahab, M. Anane, K. Riahi, N. Jedidi, Biosorption characteristics of ammonium from aqueous solutions onto *Posidonia oceanica* (L.) fibers, Desalination, 270 (2011) 40–49.

[45] H. Zheng, L. Han, H. Ma, Y. Zheng, H. Zhang, D. Liu, S. Liang, Adsorption characteristics of ammonium ion by zeolite 13X, J. Hazard. Mater., 158 (2008) 577–584.

[46] Z. Sun, X. Qu, G. Wang, S. Zheng, R.L. Frost, Removal characteristics of ammonium nitrogen from wastewater by modified Ca-bentonites, Appl. Clay Sci., 107 (2015) 46–51.

[47] A. Alshameri, H. He, J. Zhu, Y. Xi, R. Zhu, L. Ma, Q. Tao, Adsorption of ammonium by different natural clay minerals: characterization, kinetics and adsorption isotherms, Appl. Clay Sci., 159 (2018) 83–93.